IASF/CNR
Sezione di BOLOGNA
LFI Project System Team

Planck LFI

TITLE:

ELECTROMAGNETIC SIMULATIONS OF WGs VENTING HOLES

DOC. TYPE: TECHNICAL NOTE

PROJECT REF.: PL-LFI-PST-TN-042 **PAGE:** I of IV, 9

ISSUE/REV.: 1.0 **DATE:** June 2003

Prepared by	**F. CUTTAIA** **LFI** **Project System Team**	**Date:** **Signature:**	**June 10th, 2003**
Checked by	**F. VILLA** **LFI** **Project System Team**	**Date:** **Signature:**	**June 10th, 2003**
Agreed by	**C. BUTLER** **LFI** **Program Manager**	**Date:** **Signature:**	**June 10th, 2003**
Approved by	**N. MANDOLESI** **LFI** **Principal Investigator**	**Date:** **Signature:**	**June 10th, 2003**

DISTRIBUTION LIST

Recipient	Company / Institute	E-mail address	Sent
A. MAMBRETTI	LABEN – Vimodrone	mambretti.an@laben.it	YES
E. ALIPPI	LABEN – Vimodrone	alippi.e@laben.it	YES
F. MONZANI	LABEN – Vimodrone	monzani.f@laben.it	YES
P. GUZZI	LABEN – Vimodrone	guzzi.p@laben.it	YES
R.C. BUTLER	IASF/CNR – Bologna	bulter@bo.iasf.cnr.it	YES
N. MANDOLESI	IASF/CNR – Bologna	mandolesi@bo.iasf.cnr.it	YES
M. BERSANELLI	UNIMI – Milano	Marco.Bersanelli@uni.mi.astro.it	YES
LFI SPCC	IASF/CNR – Bologna	lfispcc@bo.iasf.cnr.it	YES

CHANGE RECORD

Issue	Date	Sheet	Description of Change	Release
1.0	June 10, 2003	All	First Issue of the Document	===

TABLE OF CONTENTS

1 INTRODUCTION AND SCOPE

LFI waveguides may create problem in empty out the LFI front–end modules and back–end modules during the satellite launch. In order to avoid any damage of the radiometers, holes in waveguides may be necessary to facilitate the reaching of the vacuum condition in space: the air will flow mainly through these hole instead through the radiometers.

The waveguide is a two–port transmission line. Independently on the diameter and position, an hole in the waveguide wall introduces a third port in the transmission line. Thus the hole may (i) generate reflections inside the waveguide (because it changes the impedance) and may (ii) radiates electromagnetic power into space (since it is an aperture).

In general, the hole needs to be as large as possible to evacuate the air inside the waveguide and as small as possible to avoid any perturbation of the electromagnetic field propagating inside the waveguide (this can be controlled with an appropriate location of the hole). Moreover, (i) can be limited also by an appropriate location of the hole and (ii) can be controlled making the hole depth as long as possible in order to cut off the propagation of the electromagnetic field inside the hole, provided that the hole diameter satisfy the following equation:

$$d << d_{\max} = \frac{1.841}{\pi \cdot \sqrt{\varepsilon_0 \mu_0}} \cdot \frac{1}{\upsilon_{HF}}$$

where υ_{HF} is the higher frequency can propagate in the waveguide. In the case of LFI this is set a 77 GHz and the resulting $d_{\max} \cong 2.3\,\text{mm}$.

It has been decided to propose a single hole per waveguide directly on the flange, symmetrically in the E–plane, with the hole axis parallel to the H–plane (see Figure 1). The hole diameters has been set at 1 mm.

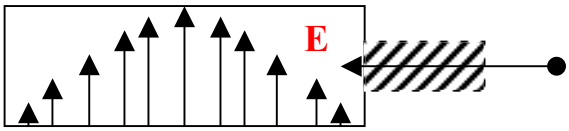

Figure 1: E-field vector representation inside a waveguide; the hole and its axis are also shown by hatch and arrow.

Purpose of this technical note is to assess the impact of venting holes on the electromagnetic performances of LFI waveguides.

The assessment of the need of venting holes for the LFI waveguide is not a purpose of the study reported here.

Simulations have been performed at 70 GHz on a straight section of the WR12 waveguide, using the Finite Elements Method based HFSS software. This frequency is the most critical one since the hole diameter is about 2/3 of the waveguide lateral dimension. Two models will be illustrated:

- the *model 1* describes the system as a three ports device; a transmitting port, a receiving port and the hole represented as the third port; it is supposed that the hole does not radiate into space.
- the *model 2* describes the system as a two ports device. The port 1 and 2 are the two ends of the waveguide; in this case the hole, considered as an aperture, radiates power in the surrounding space modelled as a radiating boundary backed by perfect matched layers.

2 REFERENCE DOCUMENTS

[RD 1] N.J. Cronin, *"Microwave and optical waveguides"*, Institute of Physics Publishing, Bristol and Philadelphia, 1995.

[RD 2] ANSOFT HFSS 8.5 User manual

3 CONSTRAINTS

The constraints assumed in this study are the following:

- The waveguide is a standard WR12 rectangular waveguide
- The dimensions of the flange is based on the drawing reported in Figure 2
- The hole is circular and the dimensions are 1 mm in diameter and 6.95 mm in depth, as derived from the flange design.
- The frequency range is set to be 63÷77 GHz,

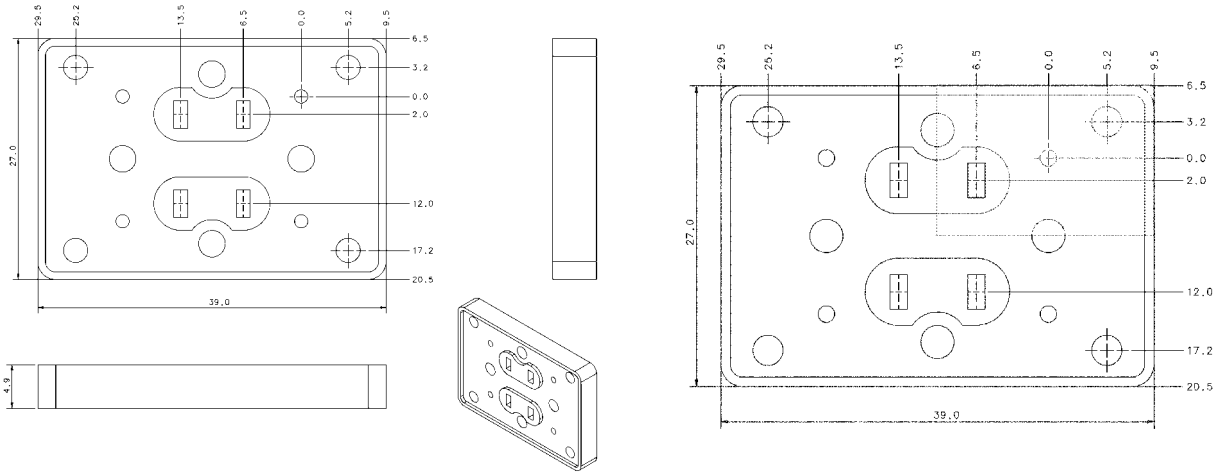

Figure 2: 70 GHz flange design adopted for these simulations (left). The electromagnetic model has been defined assuming the shadow part as reported in the right panel: ¼ of the geometry has been used.

4 MODEL 1: THREE PORTS MODEL

The waveguide is composed by two parts symmetrically placed with respect to the flange; each part was modelled as a parallelepiped with rectangular base of 3,1mm X 1,55mm and 15 mm in length.
the three ports were put on the two waveguide's apertures (port 1 and port 2) and on the hole's aperture placed on the external surface of the flange (see Figure 3).

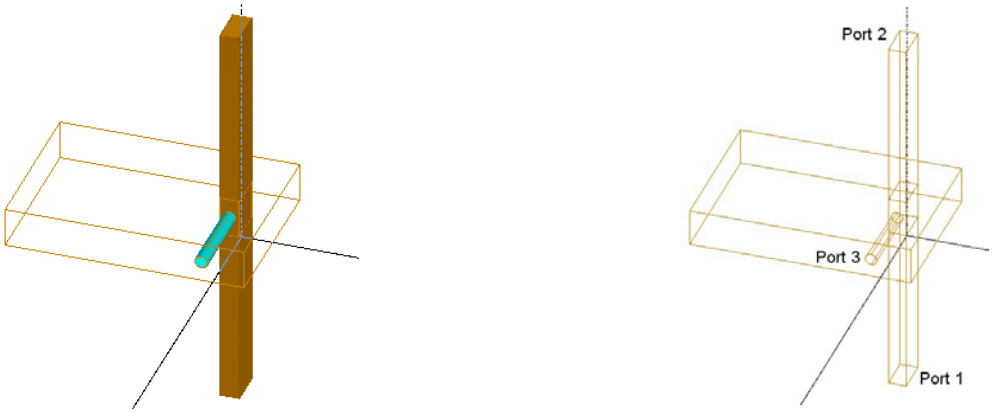

Figure 3: 3D representation of the three ports device (Model 1)

The accuracy requested for the solution has been set to $\Delta S_{ij} = \left| S_{ij}(N) - S_{ij}(N-1) \right| \le \Delta S_{MAX} = 0.001$, where N is one simulation run, S_{ij} is the scattering matrix at a given run, ΔS_{ij} is the difference between the scattering matrix at a given run (N) and the matrix at the previous run (N–1). The runs differ from the number of thetrahedra used in the simulation. In this case, the 0.1% of difference has been assumed as a upper limit for the convergence of the results, independently on the values (amplitude and phase) of the scattering parameters.
Table 1 reports the simulation time, the number of iterations, and the tetrahedra used in this simulation. In these simulations, a value of $\Delta S_{ij} = 0.00097$ was reached, as reported in Figure 4.

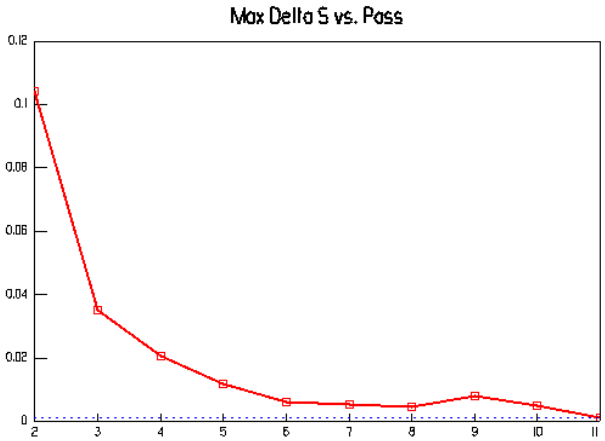

Figure 4: Maximum ΔS_{ij} versus the order of iteration is displayed; in dashed blue, the upper limit (0.001) previously set is reported.

Total time	Real time	CPU time	Iterations	Memory size	Tetrahedra
27m57s	20m31s	12m30s	11	139166K	15806

Table 1: simulation details for the model 1

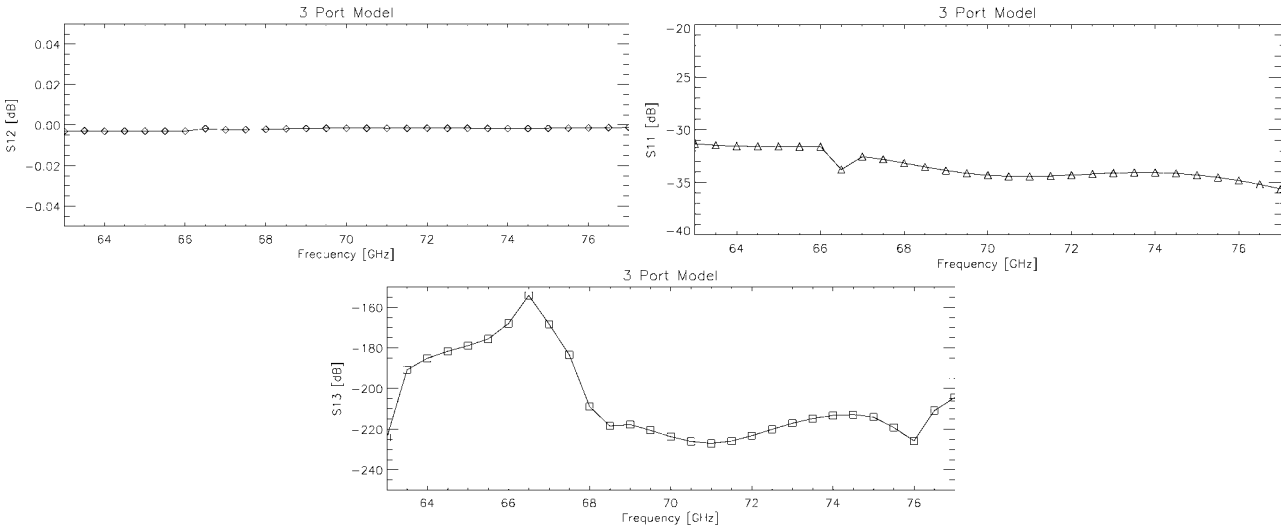

Figure 5: Scattering Parameters in dB as a function of frequency. Upper left: S12 (waveguide insertion loss). Upper right: S11 (return loss at the waveguide input port). Bottom: S13 (Insertion loss between the waveguide input port and the hole).

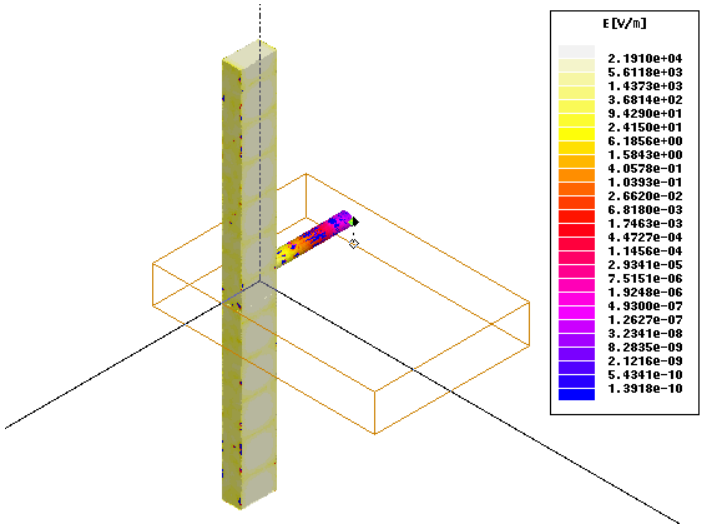

Figure 6: Coloured view of the field inside the hole.

5 MODEL 2: THE TWO PORTS RADIATING MODEL

The design model was obtained from the model 1, with some changes (see Figure 7)
A radiation box (base) was defined around the external aperture of the hole: this permits to represent the space surrounding the hole radiating aperture.
Perfect matched layers (PMLs) were located around the base (see Figure 7) to reduce spurious reflections by the radiation box. On each PML, appropriate boundary impedance conditions were set in order to simulate an infinite vacuum background.

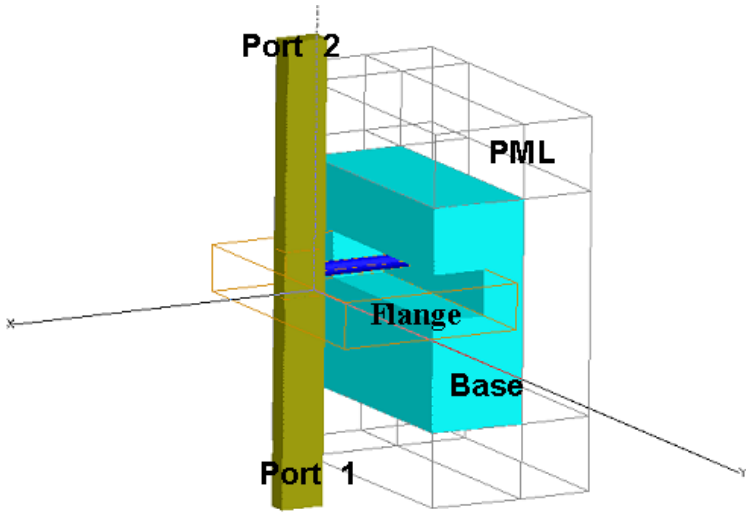

Figure 7 3-D rendered representation for the two ports model 2; in evidence as flat shaded, the waveguide (green), the hole (blue), the base (light blue); represented as wireframe are the flange (brown) and the PML boxes (grey)

The accuracy requested for the solution was the same of the model 1; after 12 iterations, the reached value for ΔS_{ij} is 0,00075.

Table 2 reports the simulation time, the number of iterations, and the tetrahedra used in this simulation.

Total time	Real time	CPU time	Iterations	Memory size	Tetrahedra
1h49m20s	56m24s	32m25s	12	480924K	30228

Table 2 simulation details for the model 2

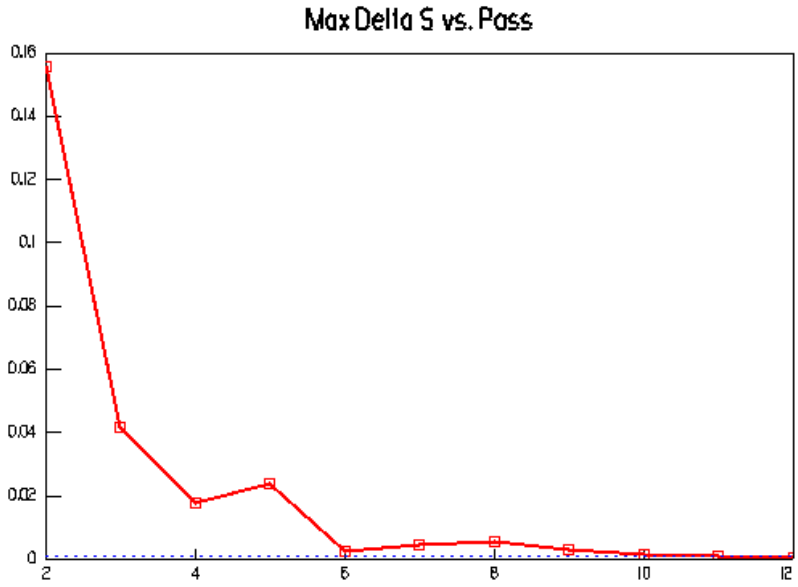

Figure 8 Maximum ΔS_{ij} versus the order of iteration is displayed; in dashed blue the upper limit for convergency (0.001) is reported.

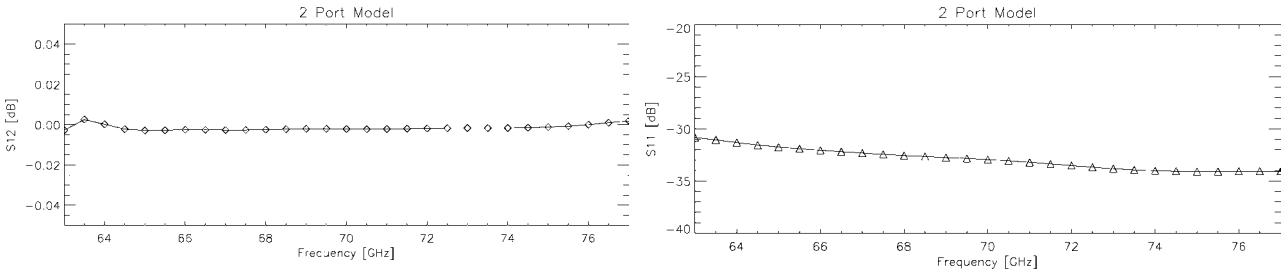

Figure 9: Scattering Parameters in dB as a function of frequency. Left: S12 (waveguide insertion loss). Upper right: S11 (return loss a the waveguide input port).

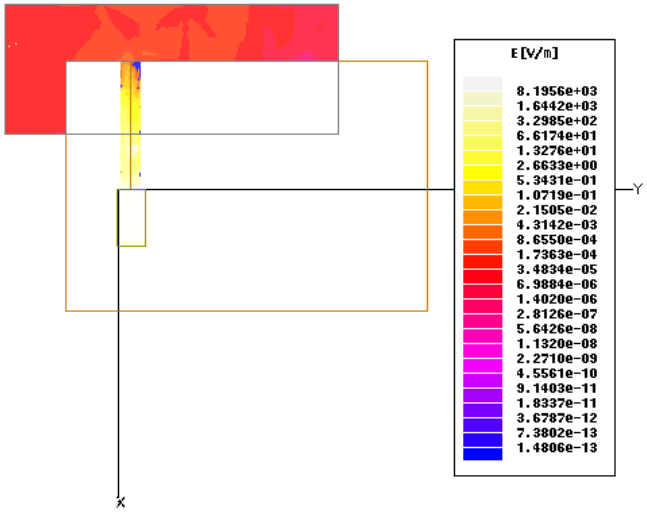

Figure 10 E-total Field representation on a cut-plane [x-y] passing trough the hole's axis. The colour scale is logarithmic

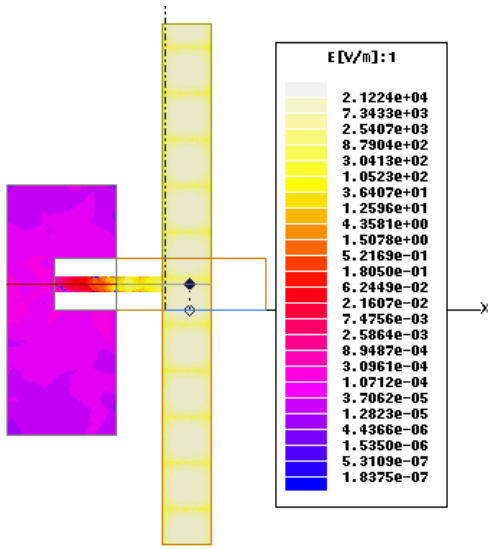

Figure 11: E-total Field representation on a cut-plane [z-y] passing trough the hole's axis. The colour scale is logarithmic

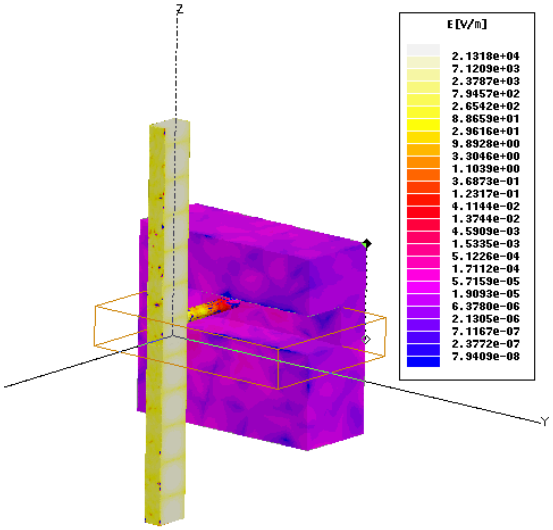

Figure 12: E-field representation on the 3D surfaces: waveguide, hole, base. The colour scale is logarithmic.

The integrated power at the radiation box has been calculated with HFSS at seven frequencies: 63, 66, 68, 70, 72, 74, and 77GHz. The average value as been calculated resulting at -161.28dB. This value can be considered as the monochromatic normalised radiated power.

6 Conclusions

The results of the simulations show that the hole studied above does not significantly impact the performances of the waveguide. The Return Loss in presence of the hole remains < –30dB (still under the requirements); the power radiated in the surrounding results at very low levels, as expected.

The comparison between the S11 and the S12 parameters (see Figure 5 and Figure 9) show that the two different method used are in good agreement. Moreover the hole average radiated power as calculated in Method 2 is consistent with the S13 parameter calculated with the Method 1.